

Non-Isolated Boost Converter with Higher Gain and Efficiency

¹Hanna George, ² Prof. Kavitha Issac, ³ Prof. Neema S, ⁴ Prof. Jeena Joy, ⁵ Prof. Deena George

¹PG Scholar, ² Associate Professor, ³ Assistant Professor, ⁴ Associate Professor, ⁵ Assistant Professor
Department of Electrical and Electronics Engineering
Mar Athanasius College of Engineering, Kothamangalam, Kerala

ABSTRACT

A high voltage gain non-isolated boost converter with switched inductor is proposed in the paper. The converter is constructed by adding an additional switched inductor to a conventional three-level-boost (TLB) converter. Conventional TLB converter is widely used in power electronics systems because of its simple structure. When compared with the conventional boost and TLB converters, the non-isolated boost converter can achieve higher voltage conversion ratio with reduced voltage and current stresses in the switches. A special feature of the converter is to automatically balance the output voltages for an unbalanced load without the need of any additional control strategy or auxiliary circuit. The converter is more suitable than the traditional TLB converter for high step-up applications. The performance study of converter is carried out with MATLAB/SIMULINK R2017a. From the analysis it is observed that the performance of the converter is improved. The converter has a maximum efficiency of 96%.

Keywords: High gain boost converter, Switched inductor cell and Non-isolated

Date of Submission: 10-03-2021

Date of Acceptance: 25-03-2021

I. INTRODUCTION

As nonrenewable resources such as oil, gas and coal become scarce in the current scenario, more researches are focused on the issue of high energy usage and society's dependence on fossil fuels [1]-[3]. Moreover, the number of automobiles continues to increase day by day in most countries, causing an immense rise in air pollution. Vehicles powered by fuel cell sources may help to reduce transport's dependence on oil, and reduce polluting emissions [4]. The fuel cells can use hydrogen or natural gas, to get a high energy density and can efficiently generate "clean" electricity with high efficiency. Unlike batteries that have a fairly constant output voltage, the output voltage of fuel cells drops down significantly with an increase in overall output current [5]-[7]. Hence, a step-up DC-DC converter with a wide range of voltage-gain is essentially needed to interface between the low voltage fuel-cell source and the high voltage DC bus of the motor drive inverter. The conventional DC-DC Boost converter is one of the most commonly used topologies for boosting up voltage. When the duty cycle approaches unity, the conventional boost converter can achieve a high voltage gain [8].

In order to improve the overall efficiency and voltage gain, other types of boost converters have been studied and investigated [6]-[8]. In [6]-

[7], the voltage conversion ratio was improved at the cost of additional components, which decreased the efficiency and increased converter volume. In [7]-[8], coupled inductors were used widely to improve the step-up function and efficiency. However, the high surge voltage caused by the leakage inductance necessitates the use of high voltage rating devices or snubber circuits. In order to overcome the above mentioned drawbacks, a three-level-boost (TLB) converter was introduced and has been used widely. The converter can be operated as either single output V_o or dual output V_{o1} , V_{o2} depending on its applications. It has several advantages over the traditional boost converter including higher voltage gain and reduced switch voltage stress than the traditional boost converter; therefore, switching and reverse recovery losses can be reduced considerably [9]-[10]. As a result, the conventional TLB converter is more suitable than the traditional boost converter for high step-up applications, including power factor correction [6], photovoltaic [8]-[9], and wind power generation [10] systems. These applications and systems primarily use the circuit topologies based on the conventional TLB converter followed by multi-level inverters, including the neutral-point-clamped inverters [6]-[8].

II. HIGH GAIN NON-ISOLATED BOOST CONVERTER

The high gain non-isolated boost converter consists of four switches S_1 , S_2 , S_3 and S_4 , three inductors L_{in} , L_1 and L_s , three diodes D_1 , D_2 and D_3 , two output capacitors C_{o1} and C_{o2} and two output resistors R_{o1} and R_{o2} . V_{in} is the input voltage and output voltage is denoted as V_o . Figure 1 shows a circuit of typical arrangement of high gain boost converter.

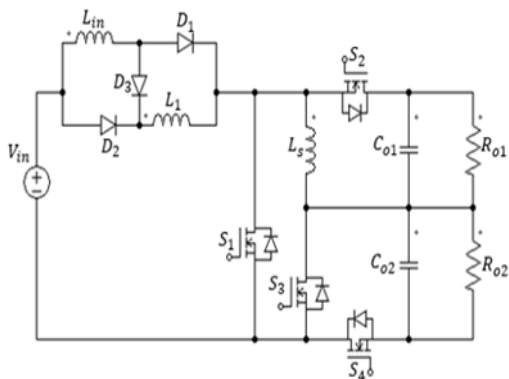


Fig. 1. High Gain Non-Isolated Boost Converter

More importantly, the proposed converter has inherent (automatic or self-correcting) output voltage balancing feature. The efficiency of the converter is improved and higher gain is obtained.

A. Modes of Operation

The working of the circuit when R_{o1} and R_{o2} are equal can be explained by 4 modes of operation.

Mode 1: In this mode, switches S_1 and S_3 are turned on and switches S_2 and S_4 are turned off. Diodes D_1 and D_2 are reverse biased and diode D_3 is forward biased. Inductors L_{in} and L_1 are charging. Figure 2(a) shows the equivalent circuit diagram and current paths for mode 1.

Mode 2: In this mode, switches S_1 and S_4 are turned on and switches S_2 and S_3 are turned off. Diodes D_1 and D_2 are reverse biased and diode D_3 is forward biased. Inductors L_{in} and L_1 are charging. Figure 2(b) shows the equivalent circuit diagram and current paths for mode 2.

Mode 3: In this mode, switches S_1 and S_3 are turned on and switches S_2 and S_4 are turned off. Diodes D_1 and D_2 are reverse biased and diode D_3 is forward biased. Inductors L_{in} and L_1 are charging. Figure 2(c) shows the equivalent circuit diagram and current paths for mode 3.

Mode 4: In this mode, switches S_2 and S_3 are turned on and switches S_1 and S_4 are turned off. Diodes D_1 and D_2 are forward biased and diode D_3 is reverse biased. Inductors L_{in} and L_1 are discharging. Figure 2(d) shows the equivalent

circuit diagram and current paths for mode 4. Figure 3 shows the theoretical waveform for all the modes.

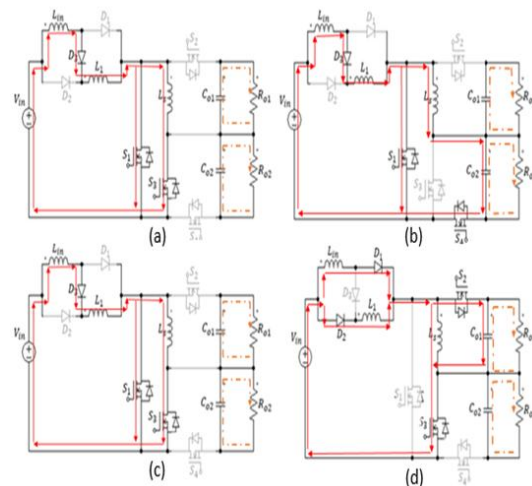


Fig. 2. Mode 1-4 ($R_{o1} = R_{o2}$)

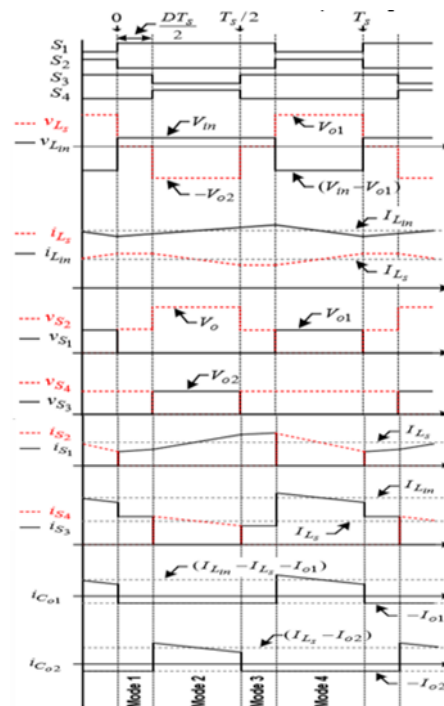


Fig. 3. Theoretical Waveform of Converter

The working of the circuit when R_{o1} varies R_{o2} fixed can be explained by 3 modes of operation.

Mode 1: In this mode, switches S_2 and S_3 are turned on and switches S_1 and S_4 are turned off. Diodes D_1 and D_2 are forward biased and diode D_3 is reverse biased. Inductors L_{in} and L_1 are discharging. In this mode $I_{L_{in}}$ is greater than I_{L_s} , thus current $I_{L_{in}} - I_{L_s}$ flows through S_2 . Therefore C_{o1} is charged by this current and V_{L_s} is equal

to V_{o1} . Figure 4(a) shows the equivalent circuit diagram and current paths for mode 1.

Mode 2: In this mode, switches S_2 and S_3 are turned on and switches S_1 and S_4 are turned off. Diodes D_1 and D_2 are forward biased and diode D_3 is reverse biased. Inductors L_{in} and L_1 are discharging. In this mode $I_{L_{in}}$ is less than I_{L_s} , thus C_{o1} is discharged by the current $I_{L_{in}} - I_{L_s}$ flowing through S_2 and V_{L_s} is equal to V_{o1} . Figure 4(b) shows the equivalent circuit diagram and current paths for mode 2.

Mode 3 : In this mode, switch S_3 is turned on and switches S_1, S_2 and S_4 are turned off. Diodes D_1 and D_2 are forward biased and diode D_3 is reverse biased. Inductors L_{in} and L_1 are discharging. In this mode $I_{L_{in}}$ is still less than I_{L_s} , thus current cannot flow through S_2 because S_2 is turned off. Instead the current $I_{L_s} - I_{L_{in}}$ flows through body diode of S_1 . During this time V_{L_s} becomes zero. Figure 4(c) shows the equivalent circuit diagram and current paths for mode 3. The waveform for all three modes are shown in Figure 5.

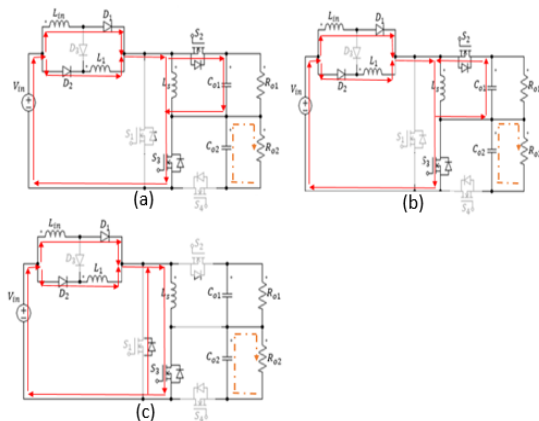


Fig. 4. Mode 1-3 (R_{o1} varies and R_{o2} fixed)

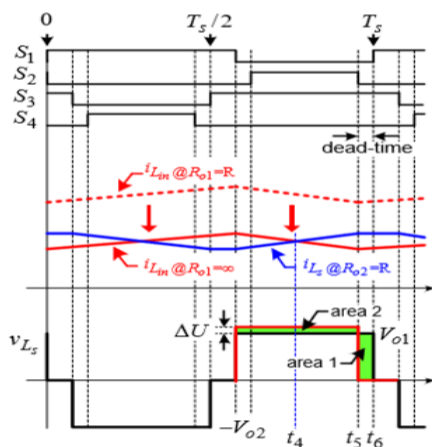


Fig. 5. Theoretical Waveform of Converter

The working of the circuit when R_{o1} fixed R_{o2} varies can be explained by 3 modes of operation.

Mode 1: In this mode, switches S_1 and S_4 are turned on and switches S_2 and S_3 are turned off. Diodes D_1 and D_2 are reverse biased and diode D_3 is forward biased. Inductors L_{in} and L_1 are charging. In this mode I_{L_s} is greater than zero, thus current I_{L_s} flows through S_4 . Therefore C_{o2} is charged by this current and V_{L_s} is equal to $-V_{o2}$. Figure 6(a) shows the equivalent circuit diagram and current paths for mode 1.

Mode 2: In this mode, switches S_1 and S_4 are turned on and switches S_2 and S_3 are turned off. Diodes D_1 and D_2 are reverse biased and diode D_3 is forward biased. Inductors L_{in} and L_1 are charging. In this mode I_{L_s} is less than zero, thus C_{o2} is discharged by this current flowing through S_4 and V_{L_s} is equal to $-V_{o2}$. Figure 6(b) shows the equivalent circuit diagram and current paths for mode 2.

Mode 3 : In this mode, switch S_1 is turned on and switches S_2, S_3 and S_4 are turned off. Diodes D_1 and D_2 are reverse biased and diode D_3 is forward biased. Inductors L_{in} and L_1 are charging. In this mode $I_{L_{in}}$ is still negative, thus current cannot flow through S_4 because S_4 is turned off. Instead the current I_{L_s} flows through body diode of S_3 . During this time V_{L_s} becomes zero. Figure 6(c) shows the equivalent circuit diagram and current paths for mode 3. The waveform for all the three modes are shown in Figure 7.

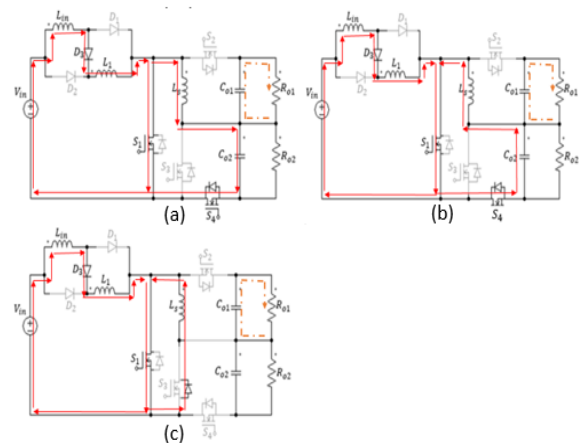


Fig. 6. Mode 1-3 (R_{o2} varies and R_{o1} fixed)

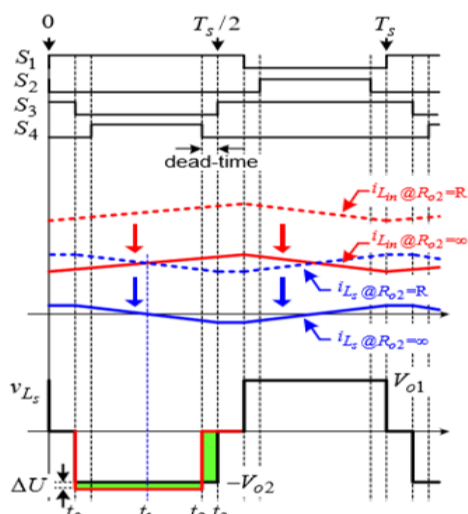


Fig. 7. Theoretical Waveform of Converter

From the above discussions it is observed that a new non isolated high voltage gain boost converter with inherent output voltage balancing is made by adding an extra inductor L_s to the conventional three level boost converter and the high gain non-isolated converter is established by adding a switched inductor to the new non-isolated high voltage gain boost converter with inherent output voltage balancing converter.

III. DESIGN OF COMPONENTS

The input voltage is taken as 120 V. Output voltage is 600V. Output current is taken as 3.3A. The pulses are switched at the rate of 50kHz.

A. Duty Ratio

$$V_o = \frac{4}{1-D} V_{in} \quad (1)$$

The value of duty ratio is 0.20

B. Resistor

Taking P_o as 2kW and output voltage as 600V, load resistance is calculated.

$$R_o = \frac{P_o^2}{V_o} = 180\Omega \quad (2)$$

The value of resistor is 180 Ω

C. Inductor

The rated output current is 3.3A. Moreover, 30% of the full load inductor current is chosen as peak to peak ripple current. The rated output voltage is 600V.

$$I_L = \frac{V_o}{R \cdot D} = 16.6 \quad (3)$$

The value of inductor current is set at 16A.

$$L_{in} = L_1 = \frac{(1-D) \cdot (1+D) \cdot V_o}{4y\% \cdot I_L \cdot 2f_s} = 2.89 \cdot 10^{-4} \quad (4)$$

The value of inductors L_{in} and L_1 is set as 280 μ H.

$$L_s = \frac{(1-D) \cdot V_o}{z\% \cdot I_L \cdot 2f_s} = 9.63 \cdot 10^{-4} \quad (5)$$

The value of inductors L_s is set as 960 μ H.

D. Capacitor

Let the output voltage be 600V. Switching

frequency is taken as 50kHz. Peak to peak output voltage ripple is to be 0.01 % of output voltage.

$$C = \frac{D}{R f_s \cdot \frac{\Delta V_o}{V_o}} = 1.87 \cdot 10^{-4} \quad (6)$$

The value of capacitor is selected as 188 μ F.

IV. SIMULATION OF THE CONVERTER WITH RESULTS

The high gain non-isolated boost converter is simulated in MATLAB/SIMULINK.

A. Simulation Results

The simulation results of the converter with equal resistances are shown in the following figures.

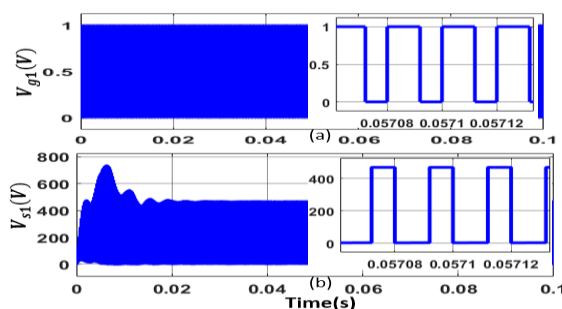


Fig. 8. (a) Gate pulse (S_1) (b) Voltage across (S_1)

Figures 8(a) and 8(b) shows the gate pulse and voltage across switch S_1 . The amplitude of switch S_1 is set as one in order to turn it on. As the switch is on, the voltage across it is 467V.

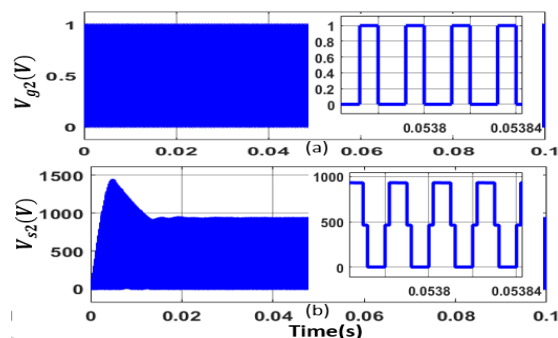


Fig. 9. (a) Gate pulse (S_2) (b) Voltage across (S_2)

Figures 9(a) and 9(b) shows the gate pulse and voltage across switch S_2 . The amplitude of switch S_2 is set as one in order to turn it on. As the switch is on, the voltage across it is 933V.

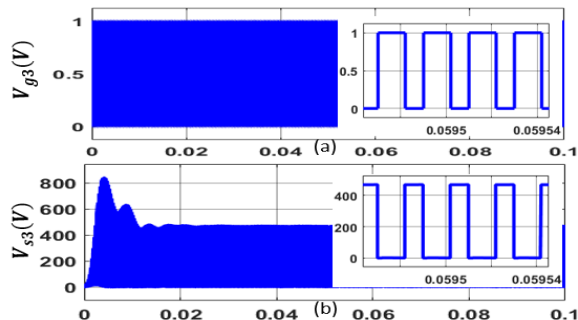


Fig. 10. (a) Gate pulse (S_3) (b) Voltage across (S_3)

Figures 10(a) and 10(b) shows the gate pulse and voltage across switch S_3 . The amplitude of switch S_3 is set as one in order to turn it on. As the switch is on, the voltage across it is 467V.

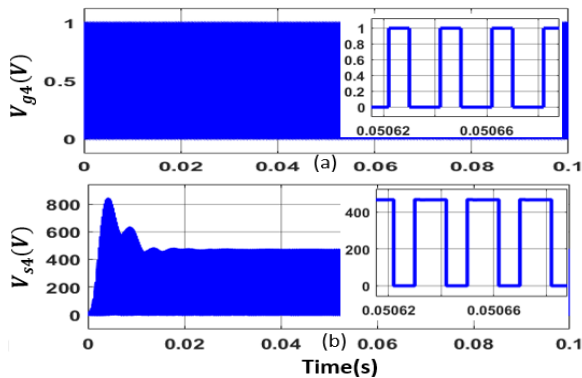


Fig. 11. (a) Gate pulse (S_4) (b) Voltage across (S_4)

Figures 11(a) and 11(b) shows the gate pulse and voltage across switch S_4 . The amplitude of switch S_4 is set as one in order to turn it on. As the switch is on, the voltage across it is 467V.

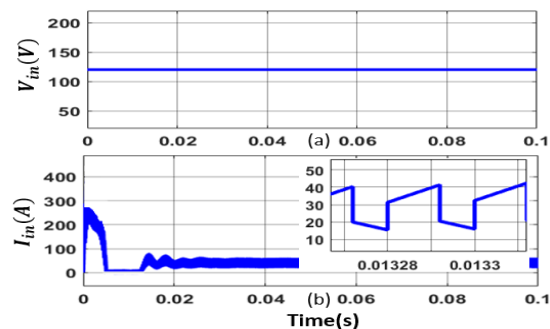


Fig. 12. (a) Input Voltage (V_{in}) (b) Input Current (I_{in})

In figure 12(a), it is seen that the input voltage to the circuit is 120V. It is a constant dc supply. Figure 12(b) shows the input current waveform. The magnitude of input current is 41A. When switch is turned on, input current starts to increase and when the switch is turned off, input

current decreases. Input current of the converter is pulsating.

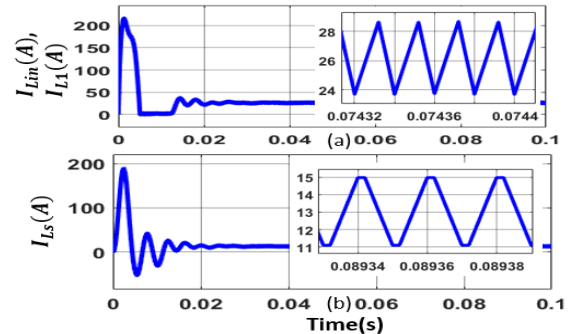


Fig. 13. Inductor Current

Figure 13 shows the inductor currents of the converter with a magnitude of 28.5A for L_{in} and L_1 with a ripple of 4A and a magnitude of 15A for L_s with a ripple of 4A. When the switch is on, inductor is in charging mode and inductor current increases. When switch is turned off, inductor discharges and inductor current starts to decrease.

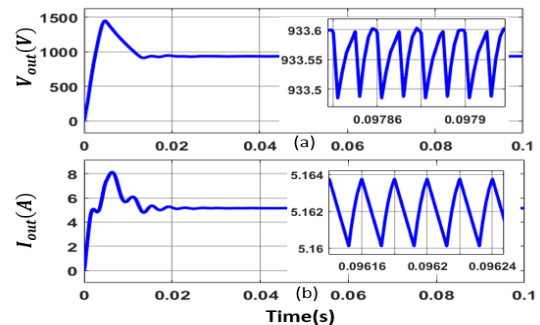


Fig. 14. (a) Output Voltage (V_{out}) (b) Output Current (I_{out})

Figure 14(a) shows the output voltage with magnitude 934V. The output voltage has a ripple of 0.15V. In boost converter the voltage is stepped up from 120V. Figure 14(b) shows the output current with magnitude 5.1A. The output current has a ripple of 0.004A.

V. ANALYSIS

The analysis of high gain non-isolated boost converter with a new non-isolated high voltage gain boost converter with inherent output voltage balancing and three level boost converter is carried out by considering parameters like voltage gain, efficiency and duty cycle.

a. Efficiency Vs Output Power

Efficiency of a power equipment is defined as any load as the ratio of the power output to the power input. The efficiency tells us the fraction of the input

power delivered to the load. A typical curve for the variation of efficiency as a function of output power is shown in Figure 15. The converter efficiency is around 96% for high gain non-isolated boost converter for R load.

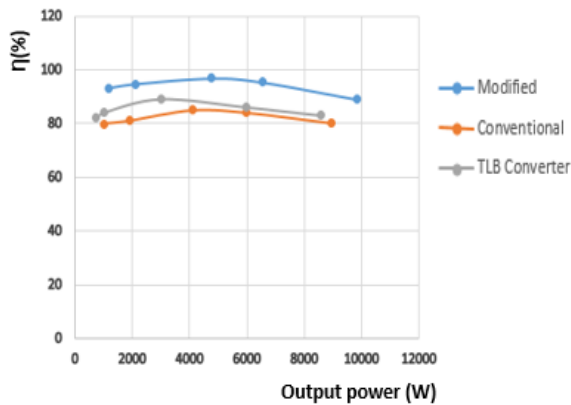


Fig. 15. Efficiency Vs load R load

b. Gain Vs Duty Cycle

The plot of voltage gain as a function of duty cycle is shown in Figure 16. According to figure, the voltage gain of boost converter is the highest when $D=0.2$ in both modified and conventional converter

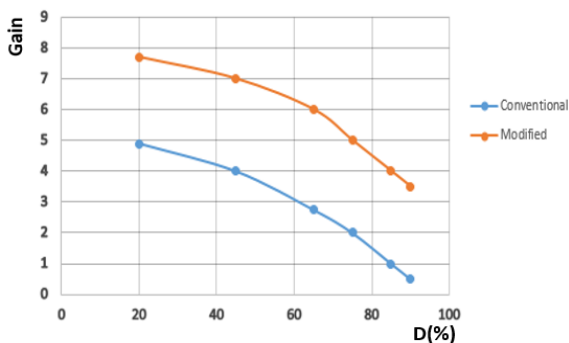


Fig. 16. Voltage gain Vs duty cycle

c. Efficiency Vs Duty Cycle

The plot of efficiency as a function of duty cycle is shown in Figure 17. According to figure, the efficiency of boost converter is more when $D=0.2$ in both modified and conventional converter.

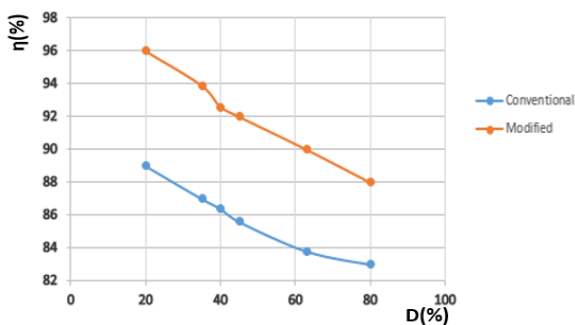


Fig. 17. Efficiency gain Vs duty cycle

d. Loss Analysis

The loss analysis of the converter is shown in Figure 18. According to figure, the losses of the non-isolated high gain boost converter with output voltage balancing is less

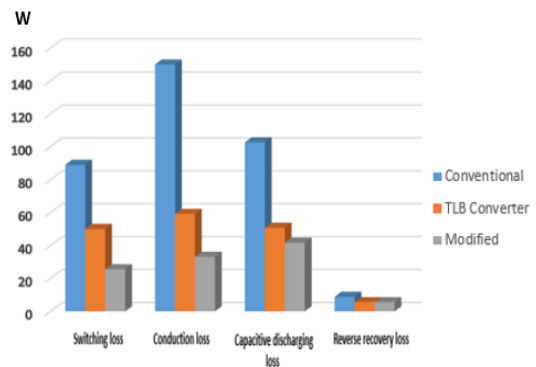


Fig. 18. Loss analysis

e. Comparison

The comparison between conventional three level boost converter, high gain boost converter with inherent output voltage balancing and high gain non-isolated boost converter is given in table 1. It is observed from the below discussions that high gain non-isolated boost converter has higher efficiency and higher gain compared with the other two converters, by keeping the input voltage constant throughout. The converter is simulated in MATLAB/SIMULINK using the corresponding designed values and the waveforms are observed for the above mentioned values. The converter is also compared with three level boost converter and conventional non-isolated boost converter.

TABLE I
COMPARISON OF DIFFERENT BOOST CONVERTERS

PARAMETERS	THREE LEVEL BOOST CONVERTER $V_{in}=120V$ $V_o=600V$	NON-ISOLATED BOOST CONVERTER $V_{in}=120V$ $V_o=600V$	HIGH GAIN NON ISOLATED BOOST CONVERTER $V_{in}=120V$ $V_o=934V$
No. of components	Switch =4 Inductor =1 Capacitor=2 Resistor =2 Diode =0	Switch =4 Inductor =2 Capacitor=2 Resistor =2 Diode =0	Switch =4 Inductor =3 Capacitor=2 Resistor =2 Diode =3
Efficiency	83.8%	89.03%	96%
Voltage gain	4.9	4.9	7.78
Voltage stress (across switches)	V_o	$\frac{V_o}{2}$	$\frac{V_o}{2}$
Duty ratio	0.6	0.2	0.2

VI. CONCLUSION

The high gain non-isolated boost converter offers a high efficiency to the converter. This converter can automatically balance the output voltages for an unbalanced load without the need of any additional control strategy or auxiliary circuit. The proposed boost converter features a switched inductor cell which increases the overall efficiency and voltage gain. The overall efficiency of the converter is 96%. The main disadvantage related with this circuit is that the number of components is relatively high due to the implementation of switched inductor cell and thereby the losses increases. The overall cost of the circuit also gradually increases. The converter can be used for a constant dc application such as traction, telecommunication, battery charging etc.

REFERENCES

- [1]. Hyemin Kang and Honnyong Cha, "A New Non- Isolated High Voltage Gain Boost Converter with Inherent Output Voltage Balancing," Transactions on Industrial Electronics, DOI 10.1109, 2018.
- [2]. G. Estay, L. Vattuone, S. Kouro, M. Duran, and B. Wu, "Dual-boostNPC converter for a dual three-phase PMSG wind energy conversion system," IEEE Int. Conf. Power Electron, Drives Energy Syst., 2012, pp. 16.
- [3]. L. Palma, M. H. Todorovic, and P. N. Enjeti, "Analysis of commonmode voltage in utility-interactive fuel cell power conditioners," IEEE Trans. Ind. Electro., vol. 56, no. 1, pp. 20 27, Jan. 2009.
- [4]. B. Lu, Y. Qiu, C. Wang, Y. Kang, J. Sun, W. Dong, F. Canales, P. Barbosa, M. Xu, F. C. Lee, R. Gean, W. C. Tipton, and D. Urciuoli, "A high power density high voltage distributed power system for pulse power applications," IEEE APEC, Austin, TX, 2005.
- [5]. D. Damasceno, L. Schuch, and J. R. Pinheiro, "Design procedure to minimize boost PFC volume concerning the trade-offs among switching frequency, input current ripple and soft-switching," IEEE PESC, 2005, pp. 23332338.
- [6]. O. Garcia, J. A. Cobos, R. Prieto, P. Alou, and J. Uceda, "Power factor correction: A survey," IEEE PESC, 2001, pp. 813.
- [7]. B. Ivanovic and Z. Stojkovic, "A novel active soft switching snubber designed for boost converter," IEEE Trans. Power Electron, vol. 19, no. 3, pp. 658665, May. 2004.
- [8]. R. J. Wai, L. W. Liu, and R. Y. Duan, "High-efficiency dedc converter with high voltage gain and reduced switch stress," IEEE Trans. Ind. Electron., vol. 54, no. 1, pp. 354364, Feb. 2007.
- [9]. X. Ruan, B. Li, Q. Chen, S. Tan, and C. K. Tse, "Fundamental considerations of three-level DCDC converters: Topologies, analyses, and control," IEEE Trans. Circuits System, vol. 55, no. 11, pp. 37333743, Dec. 2008.
- [10]. H. C. Chen and J. Y. Liao, "Design and implementation of sensor less capacitor voltage balancing control for three-level boosting PFC converter," IEEE Trans. Power Electron, vol. 29, no. 7, pp. 38083817, Jul. 2014.

AUTHOR PROFILES

HANNA GEORGE received UG degree in Electrical and Electronics Engineering from Mahatma Gandhi University and pursuing her M. Tech from Mar Athanasius College of Engineering. Her areas of interests are Power Electronics, Electric Drive, Renewable Energy, and Electric Vehicle Technology.

KAVITHA ISSAC received UG degree in Electrical and Electronics Engineering from Mahatma Gandhi University. She received PG degree in the stream of Control System from Anna University. She is currently working as Associate Professor in the department of Electrical and Electronics Engineering at Mar Athanasius College of Engineering.

NEEMA S received UG degree in Electrical and Electronics Engineering. She received PG degree in the stream of Control System. She is currently

working as Assistant Professor in the department of Electrical and Electronics Engineering at Mar Athanasius College of Engineering.

JEENA JOY received UG degree in Electrical and Electronics Engineering from Mahatma Gandhi University. She received PG degree in the stream of Control System from Anna University. Her areas of interests are Power System, Control System and Signal Processing. She is currently working as Assistant Professor in the department of Electrical and Electronics Engineering at Mar Athanasius College of Engineering.

DEENA GEORGE received UG degree in Electrical and Electronics Engineering. She received PG degree in the stream of Power Electronics. She is currently working as Assistant Professor in the department of Electrical and Electronics Engineering at Mar Athanasius College of Engineering.

Hanna George, et. al. "Non-Isolated Boost Converter with Higher Gain and Efficiency." *International Journal of Engineering Research and Applications (IJERA)*, vol.11 (3), 2021, pp 18-25.